AD_____

Award Number: W81XWH-10-1-0497

TITLE: Regulation of Mammary Tumor Formation and Lipid Biosynthesis by Spot14

PRINCIPAL INVESTIGATOR: Elizabeth Wellberg, Ph.D.

CONTRACTING ORGANIZATION: University of Colorado-Anschutz Medical Campus
Aurora, CO 80045-2505

REPORT DATE: June2014

TYPE OF REPORT: Annual Summary (Final Progress Report)

PREPARED FOR: U.S. Army Medical Research and Materiel Command
Fort Detrick, Maryland 21702-5012

REPORT DOCUMENTATION PAGE

Form Approved
OMB No. 0704-0188

1. REPORT DATE	2. REPORT TYPE	3. DATES COVERED
June 2014	Annual Summary (Final Report)	15-Sept-2010-31Mar2014

4. TITLE AND SUBTITLE

Regulation of Mammary Tumor Formation and Lipid Biosynthesis by Spot 14

5a. CONTRACT NUMBER

5b. GRANT NUMBER
W81XWH-10-1-0497

5c. PROGRAM ELEMENT NUMBER

6. AUTHOR(S)

Elizabeth Wellberg

E-Mail: Elizabeth.Wellberg@ucdenver.edu

5d. PROJECT NUMBER

5e. TASK NUMBER

5f. WORK UNIT NUMBER

7. PERFORMING ORGANIZATION NAME(S) AND ADDRESS(ES)

University of Colorado-Anschutz Medical Campus

Aurora, CO 80045-2505

8. PERFORMING ORGANIZATION REPORT NUMBER

9. SPONSORING / MONITORING AGENCY NAME(S) AND ADDRESS(ES)
U.S. Army Medical Research and Materiel Command
Fort Detrick, Maryland 21702-5012

10. SPONSOR/MONITOR'S ACRONYM(S)

11. SPONSOR/MONITOR'S REPORT NUMBER(S)

12. DISTRIBUTION / AVAILABILITY STATEMENT
Approved for Public Release; Distribution Unlimited

13. SUPPLEMENTARY NOTES

14. ABSTRACT

Spot14 (S14), encoded by the THRSP gene, regulates de novo fatty acid synthesis in the liver, adipose, and lactating mammary gland. S14 has recently been shown to stimulate FASN activity, increasing the synthesis of medium chain fatty acids in mammary epithelial cells in vivo. Elevated de novo fatty acid synthesis is a distinguishing feature of many solid tumors compared to adjacent normal tissue. This characteristic is thought to be acquired during tumor progression, as rapidly proliferating cancer cells have a heightened requirement for membrane phospholipids. Further, overexpression of fatty acid synthase (FASN) in vivo was sufficient to stimulate cell proliferation. While many studies have focused on the FASN enzyme in cancer biology, few studies have addressed the roles of proteins that modify FASN activity, such as S14. Synthesis of de novo fatty acids was modulated using two mouse models, MMTV-Neu mice overexpressing S14 and MMTV-PyMT mice lacking S14, and effects of activated or impaired fatty acid synthesis on tumor latency, growth, metastasis, and signal transduction were investigated. We evaluated S14-dependent gene expression profiles in these mouse models by microarray and used publicly available microarray datasets of human breast tumors. Here, we show that S14 overexpression in the MMTV-Neu transgenic model stimulated medium-chain fatty acid synthesis, increased proliferation and shortened tumor latency, but reduced tumor metastasis. Loss of S14 in the MMTV-PyMT model was associated with reduced levels of medium-chain fatty acids but did not alter tumor latency. Impaired fatty acid synthesis was associated with reduced solid tumor cell proliferation, the formation of cystic lesions in some animals, and decreased phosphorylation of Src and Akt. Analysis of gene expression in these mouse models and human tumors revealed a relationship between S14 status and the expression of genes associated with luminal epithelial differentiation.

15. SUBJECT TERMS
mammary tumor, breast cancer, Spot 14, lipid synthesis

16. SECURITY CLASSIFICATION OF:			17. LIMITATION OF ABSTRACT	18. NUMBER OF PAGES	19a. NAME OF RESPONSIBLE PERSON
a. REPORT	b. ABSTRACT	c. THIS PAGE			USAMRMC
U	U	U	UU	30	19b. TELEPHONE NUMBER *(include area code)*

Table of Contents

Introduction:

THRSP/Spot14/S14 is a small cytoplasmic protein that is highly expressed in tissues that synthesize fatty acids de novo. This includes the liver, adipose tissue, and the lactating mammary gland. In the liver, S14 inhibits de novo fatty acid synthesis, but it is required in adipocytes for de novo fatty acid synthesis. $S14^{-/-}$ lactating mice produce milk with reduced fatty acid content and nurse offspring with runted development. It has become increasingly clear that tumors display alterations in de novo fatty acid synthesis. Specifically, the enzyme fatty acid synthase (FASN) is often elevated in solid tumor types compared to surrounding normal tissue. High rates of fatty acid synthesis are thought to provide a survival, growth and metastatic advantage to cancer cells. S14 was reported to correlate with a poor patient outcome for women with breast cancer. Based on the role of fatty acid synthesis in cancer, the role of S14 in normal mammary biology, and the effect S14 potentially had on breast cancer outcome, we hypothesized that S14 overexpression in tumors would stimulate fatty acid synthesis, which would promote tumor growth and metastasis. We further hypothesized that S14 loss in tumors would delay tumorigenesis, reduce tumor growth and metastasis, and decrease tumor fatty acid synthesis. Until this study, nobody had demonstrated a causal link between S14 and mammary tumorigenesis. To establish this link, we have generated a mouse model in which the MMTV promoter drives the mammary specific expression of S14. These mice have been crossed with well-characterized MMTV-Neu mice, which develop mammary tumors with a long latency. We have also crossed the $S14^{-/-}$ mice with MMTV-PyMT mice to examine the effects of S14 loss on an aggressive model of mammary tumorigenesis. In this report, we summarize the studies conducted during the award period and demonstrate that S14 overexpression in MMTV-Neu mammary glands does indeed promote tumor formation, growth, and fatty acid synthesis. Interestingly, tumors emerging from S14-transgenic mice are not metastatic. Furthermore, S14 loss from MMTV-PyMT tumors slows their growth rates and reduces tumor fatty acid synthesis. In summary, we suggest that S14 regulates mammary tumor fatty acid synthesis, and therefore indirectly impacts tumor signaling pathway activation, proliferation, and metastasis. This is the first study to examine a role for S14 in regulating mammary tumorigenesis in vivo.

Body:

I have described the studies performed to date in detail below, but to avoid formatting problems, I have chosen to put all of the described figures at the end of the document.

From SOW: Specific Aim 1*: Determine the effect of Spot14 loss on the growth and metabolism of mammary tumors in vivo in MMTV-Polyomavirus Middle T Antigen (PyMT) mice.*

Task 1 (Year 2 Months 9-12) We will generate MMTV-PyMT Spot14+/+ (Control) and MMTV-PyMT Spot14-/- (Spot14 null) female mice. These mice will be used for a tumor study, and have an average tumor latency of less than 8 weeks. We expect to generate enough females for our tumor study by the end of the second year.

Task 2 (Year 3 Months 1-6) We will monitor Control and Spot14-/- females for tumor formation and will harvest tissue when the tumor reaches 1 cm. Since the MMTV-PyMT model promotes tumor formation by 6 weeks, and most tumors reach 1 cm by 12 weeks, we expect to complete this aim by the middle of year 3.

Task 3 (Year 2 Months 6-9) The preserved tumor samples collected from the recipient mice will be analyzed using qPCR, western blot, MRS, and immunohistochemistry. We anticipate completing this task by month 9 in the 3rd year.

Milestone 1: Completion of Specific Aim 1 and preparation of manuscript for publication.

Although this was originally stated to be "milestone 1", because we have changed the SOW, we now expect this to be milestone 2, and to be completed by the end of the proposal funding period.

Results from Specific Aim 1:

Based on the reported link between Spot14 overexpression and increased breast cancer cell proliferation, we hypothesized that loss of Spot14 would delay mammary tumor latency. We used MMTV-PyMT mice to study the effects of Spot14 loss because they develop mammary tumors at a young age, providing an opportunity to observe the expected delay in tumor latency. To generate MMTV-PyMT/Spot14$^{-/-}$ mice (herein referred to as PyMT/S14$^{-/-}$), MMTV-PyMT males were crossed with Spot14$^{-/-}$ female mice to produce Spot14$^{+/-}$ offspring, and those male offspring carrying the PyMT transgene were crossed with Spot14$^{+/-}$ female mice. This generated offspring carrying the PyMT transgene that were Spot14$^{+/+}$, Spot14$^{+/-}$, or Spot14$^{-/-}$. Spot14$^{+/-}$ mice were not analyzed in this study.

All PyMT mice, and approximately 50% of PyMT/S14$^{-/-}$ mice in our study formed multiple, large, solid tumors (Figure 1A and 1B). In the remaining PyMT/S14$^{-/-}$ mice, however, we observed large cystic structures (Figure 1C). Once they emerged, these cysts rapidly filled with fluid, such that the volume of the tumor expanded to 500 mm^3 in less than a week (data not

shown). The median time to palpable tumor formation in PyMT control female mice was 61 days, while the median time to palpable tumor formation in PyMT/S14$^{-/-}$ female mice was 64 days (Figure 1D). Solid tumors lacking Spot14 expression grew significantly slower than PyMT tumors (Figure 1E). S14 expression in tumors was confirmed by qPCR, and expression of Krt18 was examined as a control (Figure 1F and 1G).

Mammary glands were collected from PyMT and PyMT/S14$^{-/-}$ females and visualized as whole mounts, to compare the formation of early mammary tumors and the structure of the mammary ductal tree. Interestingly, we observed striking differences in the mammary gland structures between PyMT and PyMT/S14$^{-/-}$ mice. As previously reported [1], PyMT mice initially developed mammary tumors near the nipple region, while some hyperplastic structures could be observed in the middle and at the distal ends of the mammary glands (Figure 2A). By the time PyMT animals were 10 weeks old, the majority of the mammary gland was filled with hyperplastic epithelial structures and very few normal ducts remained (Figure 2A and 2C). In contrast, PyMT/S14$^{-/-}$ mice formed large, dilated, fluid-filled structures and we observed few solid hyperplasias in 10-week old females (Figure 2B and 2D). Analysis of Ki67 staining revealed a significant decrease in cell proliferation throughout the gland in PyMT/S14$^{-/-}$ mice, while no differences were observed in apoptotic cells between PyMT and PyMT/S14$^{-/-}$ mice at any age (Figure 2E and data not shown). Together, these data suggest that Spot14 expression is required for the robust proliferation induced by the PyMT oncogene in the mammary glands of young mice.

The growth of PyMT tumors is highly dependent on signaling through Src and the PI3K/Akt pathways [2]. When we compared solid tumors from PyMT mice to those from PyMT/S14$^{-/-}$ mice, we observed a decrease in the phosphorylated levels of Src and Akt in tumors lacking S14, suggesting that signaling through these pathways was reduced (Figure 3). Two of the three PyMT tumors shown appeared to have higher levels of phosphorylated Erk1/2 than PyMT/S14-/- tumors; however, these differences were not quantified. PyMT was expressed in all tumors examined (Figure 3A). No differences in the phosphorylation of the adapter protein Shc were observed, nor did there appear to be significant differences in the phosphorylation of the p85 subunit of PI3' kinase (data not shown). These data suggested that the decreased proliferation observed in the PyMT-induced tumors lacking S14 results from changes the signaling pathways involving both Src and Akt.

One study reported that treating MMTV-PyMT mice with the Src inhibitor SKI-606 resulted in the formation of cystic lesions that were similar in appearance to those forming in the PyMT/S14$^{-/-}$ mice [3]. Notably, we observed decreases in Src phosphorylation in these tumors compared to PyMT controls. The lesions forming in animals treated with SKI-606 were found to produce β-casein protein; therefore, we evaluated the expression of casein genes in PyMT tumors and in both solid and cystic tumors from PyMT/S14$^{-/-}$ mice. Surprisingly, we found that the cystic lesions from PyMT/S14$^{-/-}$ mice expressed significantly lower levels of Csn2 and Csn1s2a, compared to the solid tumors from those mice or to the PyMT tumors (Figure 3B). Keratin 18

expression was not different between groups (Figure 3B). Thus, while the lesions appear similar to those in SKI-606 treated mice, they likely have distinct molecular characteristics.

Lung tissue was collected from all PyMT and PyMT/S14$^{-/-}$ mice, as well as from Neu and Neu/S14 mice, to examine metastases. There were no differences in either the number of mice with lung metastases (Figure 4A) or in the number of lesions per lung between PyMT and PyMT/S14$^{-/-}$ mice (Figure 4B). Representative images of lung metastases are shown in Figure 4C and 4D.

Microarray analysis was performed to better characterize the differences between tumors from PyMT and PyMT/S14$^{-/-}$ mice. After identifying genes that were significantly differentially expressed between groups (PyMT vs PyMT/S14$^{-/-}$), we performed gene ontology (GO) enrichment and pathway analyses to identify the gene networks that were impacted by S14 loss.

Among the significantly enriched gene ontology terms in PyMT/S14$^{-/-}$ versus PyMT tumors were those involved with glucose metabolism, protein kinase activity, and cell proliferation (Table 1). KEGG pathway analysis of these tumors was consistent with these terms, showing enrichment in glycolysis/gluconeogenesis, the pentose phosphate pathway, and the cell cycle in PyMT/S14$^{-/-}$ versus PyMT tumors (Table 2).

We have recently shown that addition of S14 to recombinant fatty acid synthase enhances the production of medium chain fatty acids in vitro [4]. To determine whether the loss of S14 from mammary tumors altered the amount of fatty acids present, GC-Mass Spectrometry was used to evaluate the fatty acid profile of tumors from PyMT versus PyMT/S14$^{-/-}$ mice. We found decreased levels of many fatty acids. The largest decrease in tumor fatty acids was seen in those with chain lengths $\leq$ 16 carbons, while more modest decreases were seen in fatty acids greater than 16 carbons (Figure 5 and Table 3).

In summary, the studies performed under Specific Aim 1 have identified that S14 is required for the robust tumor growth observed in MMTV-PyMT mice. While S14 loss did not prevent tumorigenesis altogether, it did lead to slower growing solid tumors and to the formation of cystic lesions. These lesions expressed lower levels of casein genes compared to the solid tumors and to the PyMT control tumors, suggesting that they have a distinct molecular profile. Casein genes are expressed in well-differentiated mammary epithelial cells. Tumors that have features of advanced luminal epithelial differentiation are less likely to be metastatic; however, we observed equivalent metastases in both PyMT and PyMT/S14$^{-/-}$ mice. The MMTV-PyMT model is an aggressive one that is characterized by multiple tumors throughout all glands in mice, which can appear as early as 4-5 weeks of age. Because of this, it is difficult to trace the metastatic lesion to its primary tumor source. In the future, it would advantageous to transplant single lesions from PyMT/S14$^{-/-}$ donor females into recipient mice to study the metastatic behavior of the cystic tumors in an isolated environment.

Because of their unique phenotype, the cystic tumors were not evaluated in depth for their gene expression profiles, signaling pathway activation, or fatty acid contents. Instead, we performed the majority of experiments on the solid tumors from both groups of mice. We found that the loss of S14 was associated with reduced proliferation and growth rates, decreased signaling through the Src and Akt pathways, decreased levels of medium-chain fatty acids ($C \leq 16$ carbons), and reduced expression of genes in glucose metabolic networks. Based on these results, we hypothesize that S14 regulates the production of medium chain fatty acids in tumor tissue and that these fatty acids control many aspects of tumor biology. The decreased expression of metabolic genes associated with S14 loss likely reflects the slower growth rates of the tumors. Future studies examining the contribution of medium chain fatty acids to tumor signaling pathway activation will be important.

From SOW: Specific Aim 2: *Determine the effect of S14 overexpression on the onset, growth, metastasis and metabolism of mammary tumors arising in the MMTV-ErbB2 mice by generating MMTV-ErbB2, MMTV-Spot14 bitransgenic mice.*

Task 1 (Year 1 Months 1-6): We will breed the MMTV-Spot14 and MMTV-c-ErbB2 mice to generate the single and bi-transgenic offspring that will be used in our studies. We anticipate completing this task by the end of the second quarter of the first year.

Task 2 (Year 1 Month 6-Year 2 Month 6): The MMTV-Spot14, MMTV-c-ErbB2, and MMTV-Spot14/MMTV-c-ErbB2 mice will be monitored for tumor onset and growth. The tumors will be evaluated as described in the project proposal and the animals will be sacrificed when the tumor reaches 0.5 cm in diameter. The tumor and other tissues will be harvested and preserved. We anticipate completing this aim in the second quarter of the second year.

Task 3 (Year 3 Months 1-6): The tumor and other tissue samples will be analyzed using qPCR, western blot, MRS, and immunohistochemistry. These analyses will also help us determine the effect of Spot14 on tumor cell metastasis, as lung tissues will be evaluated for the presence of mammary cancer cells. We anticipate completing this task by the second quarter of the third year.

Results from Specific Aim 2:

To determine the effects of Spot14 overexpression on tumor latency, we crossed MMTV-Spot14 transgenic female mice with male MMTV-Neu mice. MMTV-Neu mice develop tumors with a longer latency than MMTV-PyMT, with the median time to tumor formation reported to be more than 200 days [5]. As expected, overexpression of S14 in MMTV-Neu mice significantly shortened tumor latency (Figure 6A), with median times to palpable tumor formation of 238 days and 279 days in Neu/S14 bitransgenic and Neu control mice, respectively. Most Neu mice developed one or two tumors per animal, and this was not affected by Spot14 overexpression (Figure 6B). Tumor cell proliferation was modestly, but significantly increased in Neu/S14 compared to Neu mice (Figure 6C).

Lung tissue was collected from Neu and Neu/S14 mice, to examine metastases. Approximately 35% (6/17) of Neu mice had metastatic lesions in their lungs (Figure 7A). Surprisingly, only 7% (1/15) of Neu/S14 mice had lung metastases (Figure 7A). Representative lung lesions are shown in Figure 7B and 7C. A close examination of primary tumors revealed evidence of lympho-vascular invasion (LVI) in 3 Neu mice (data not shown), yet no LVI was observed in Neu/S14 mice.

Microarray analysis was performed to better characterize the differences between tumors from Neu and Neu/S14 mice. After identifying genes that were significantly differentially expressed between Neu and Neu/S14 mice, we performed gene ontology (GO) enrichment and pathway analyses to identify the gene networks that were impacted by S14 overexpression.

We found enrichment of genes involved with protein translation, regulation of proliferation, and mitochondrial metabolism (Table 4). KEGG pathway analysis of Neu/S14 versus Neu tumors revealed changes in genes associated with ribosome function and oxidative phosphorylation (Table 5). These data provide evidence that modulating S14 levels in tumors impacts cell metabolism and proliferation. Overall, the observed differences in gene expression pathways are consistent with the differences in tumor growth rates and cell proliferation resulting from S14 loss or overexpression in both mouse models.

A detailed analysis of the list of significantly different genes between Neu and Neu/S14 mice, allowed us to identify several genes known to be elevated in the mammary glands of lactating versus pregnant female mice that were expressed at a higher level in tumors from the Neu/S14 mice (Figure 8). The genes associated with lactation that were overexpressed in the Neu/S14 tumors included Csn2, Csn1s1, and Csn1s2a. Interestingly, the increased expression of casein genes in the Neu/S14 tumors is consistent with the decreased expression of these same genes in PyMT/S14$^{-/-}$ tumors. The MMTV-S14 mice do not display features of precocious differentiation at any developmental timepoint, such as elevated casein genes or lobuloalveolar development [4]; therefore, we do not believe that S14 regulates differentiation *per se*. Rather, we hypothesize that S14 may be important for the survival and/or proliferation of a well-differentiated cell type in the mammary epithelium that is the target of oncogenic transformation in the Neu and PyMT models. Consistent with this is the observation that S14 (reported as Thrsp) was lost as PyMT tumors progressed from well-differentiated ademonas to aggressive carcinomas [6]. We found that one of the most significantly elevated genes in Neu/S14 tumors was Elf5, a transcription factor that regulates alveolar differentiation during pregnancy in the mouse mammary gland [7]. Recently, Elf5 was shown to repress an EMT-like phenotype during normal mammary gland development and to prevent metastasis in two mouse models of mammary tumorigenesis [8]. Thus, the observed increase in Elf5 and other genes associated with mammary lactogenic differentiation in the Neu/S14 tumors could explain the reduced metastasis seen in those mice.

Analysis of a panel of human breast cancer cell lines revealed that S14 expression was highest in those representing the luminal subtype compared to those cell lines with basal characteristics

(Figure 9A). To determine whether S14 is associated with a particular subtype of human breast tumors, we analyzed publicly available microarray data. We found that tumors with high S14 expression were significantly more likely to be luminal than basal, when considering the intrinsic subtype [9], and were also significantly more likely to be ER+ than ER- (Figure 9B and 9C). Because the gene expression profile of the Neu/S14 tumors was reminiscent of the differentiated mammary gland, we examined the non-tumor bearing mammary glands from age-matched (10 month old), and diestrus-staged Neu and Neu/S14 females. We were surprised to observe the increased presence of hyperplastic epithelial structures in Neu/S14 mice compared to Neu controls (Figure 10). Further investigation into the connection between S14 and features of luminal differentiation in human breast tumors is warranted.

GC-Mass Spectrometry was used to evaluate the fatty acid profile of tumors from Neu and Neu/S14 mice (Figure 11 and Table 3). Compared to Neu tumors, those overexpressing S14 (Neu/S14) had higher levels of fatty acids, with the greatest increase seen in those with chain lengths $\leq$ 16 carbons. These results are consistent with those from the PyMT study, which showed that S14 loss from mammary tumors decreased the levels of medium chain fatty acids (C $\leq$ 16 carbons).

From SOW: Specific Aim 3: *Determine the changes in the expression metabolic enzymes affected by gain or loss of Spot14 function in mammary tumors using microarray analysis.*

Task 1 (Year 1 Months 9-12): We will perform cDNA microarray analysis on tumor samples from the xenotransplantation of S14-/- and WT transformed mammary epithelial cells described in specific aim 1. We will also determine which pathways are affected by analyzing changes in the expression of specific genes associated with tumor cell metabolism. We anticipate completing this task by the last quarter of the first year.

Task 2 (Year 3 Months 1-12): We will perform cDNA microarray analysis on tumor samples from transgenic mice expressing ErbB2, Spot14, or both ErbB2 and Spot14 in the mammary epithelium. This will allow us to identify changes in the expression of specific metabolic pathways modulated by Spot14 using bioinformatics analysis. We anticipate completing this task and this aim by the last quarter of the third year.

Please note that the results from Specific Aim 3 are presented above within Specific Aims 1 and 2.

Milestone 2: Completion of Specific Aims 2 and 3 and preparation of manuscripts for publication.

Initially, we prepared a portion of this work for publication at the end of year 2. While we felt the study was complete, the reviewers wanted to see additional mouse work to solidify the results. Therefore, we completed the additional mouse studies and combined the results of both

into one manuscript. This manuscript is finalized and is currently under review at Breast Cancer Research.

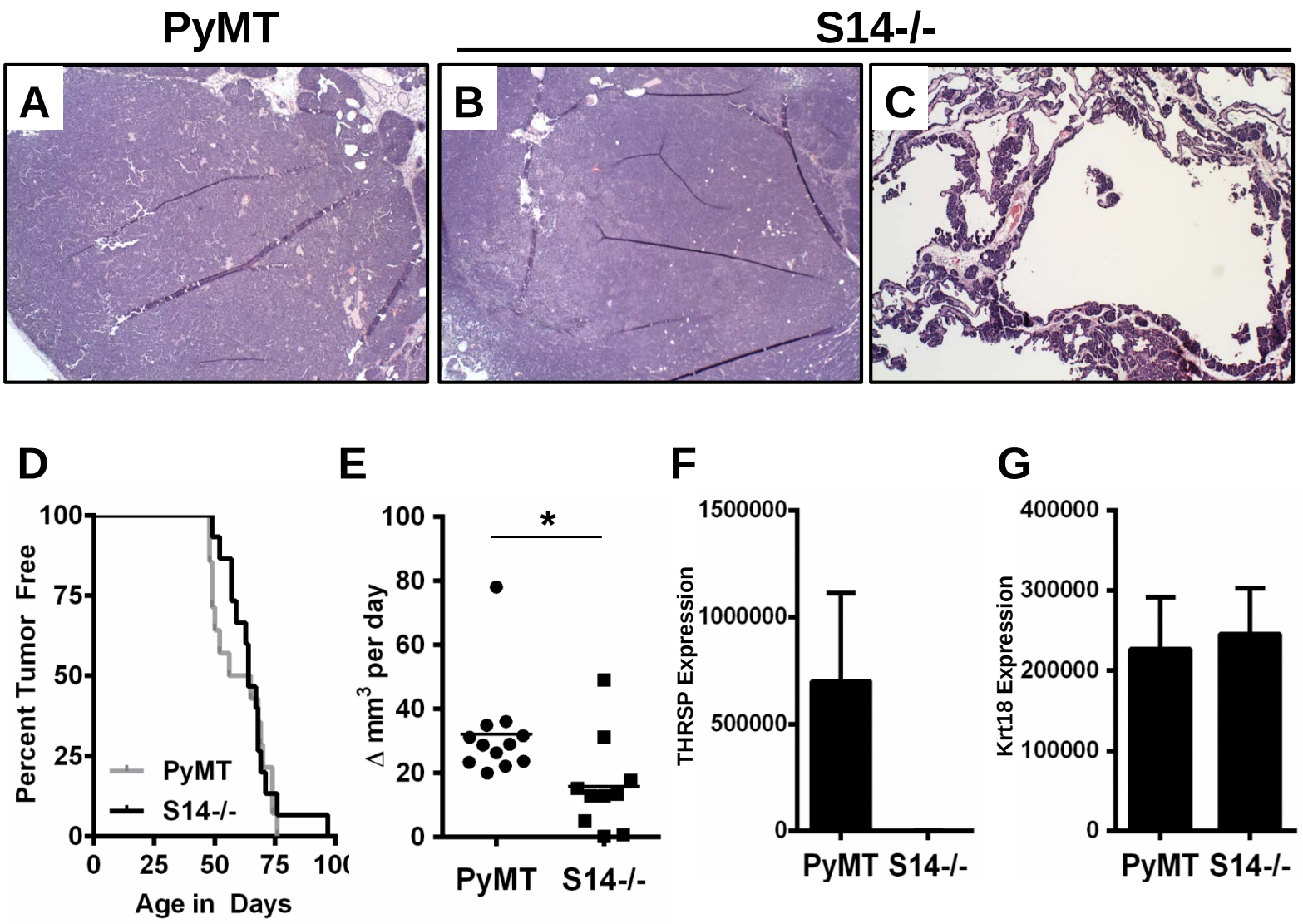

Figure 1. Tumor histology, latency, and growth in PyMT mice with and without S14. H&E stained sections of tumors from PyMT (A), and PyMT/S14$^{-/-}$ (S14$^{-/-}$) mice (B, C). A representative solid tumor is shown in (B). A tumor with a cystic morphology is shown in (C). Images were captured at 10x magnification. D) Kaplan Meier survival curve; tumors appeared with median latencies of 61 days (PyMT) and 64 days (S14$^{-/-}$; HR 1.187 (0.588-2.55); Log rank pvalue=0.62. E) Tumor growth rates; * p=0.02. F) Expression of S14 (THRSP) and (G) keratin 18 (Krt18) in tumors, measured as transcript copies in 50 ng RNA.

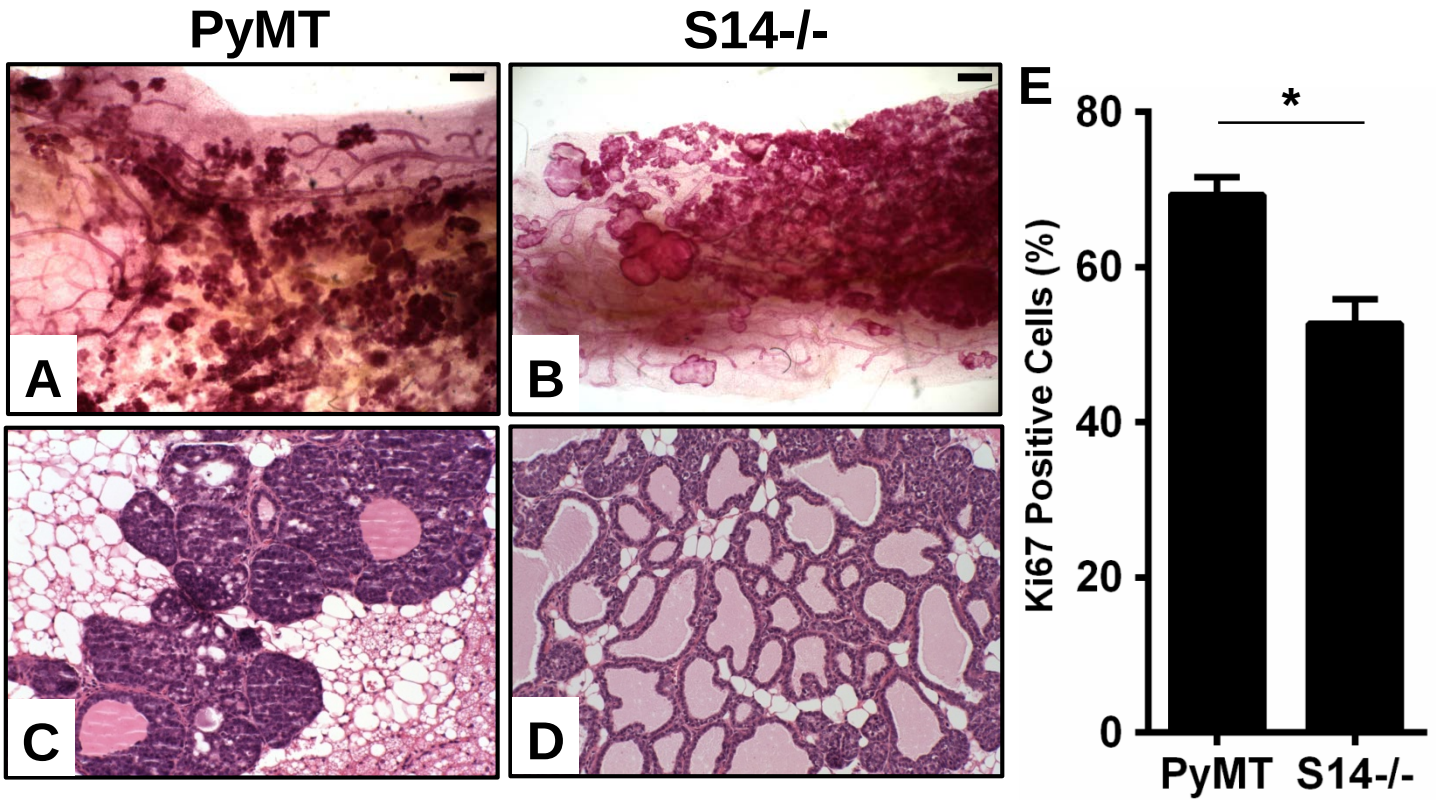

Figure 2. Mammary gland morphology and proliferation in PyMT and PyMT/S14$^{-/-}$ mice. Whole mounted mammary glands from 10 week old PyMT (A) and PyMT/S14$^{-/-}$ (S14$^{-/-}$) (B) female mice. Scale is 500 µm. H&E stained sections of mammary glands from PyMT (C) and S14$^{-/-}$ (D) mice, captured at 20x magnification. E) Quantification of Ki67 IHC (number of positive nuclei out of total) in mammary glands from10 week old mice. N=5 mice per group; $p<0.005$

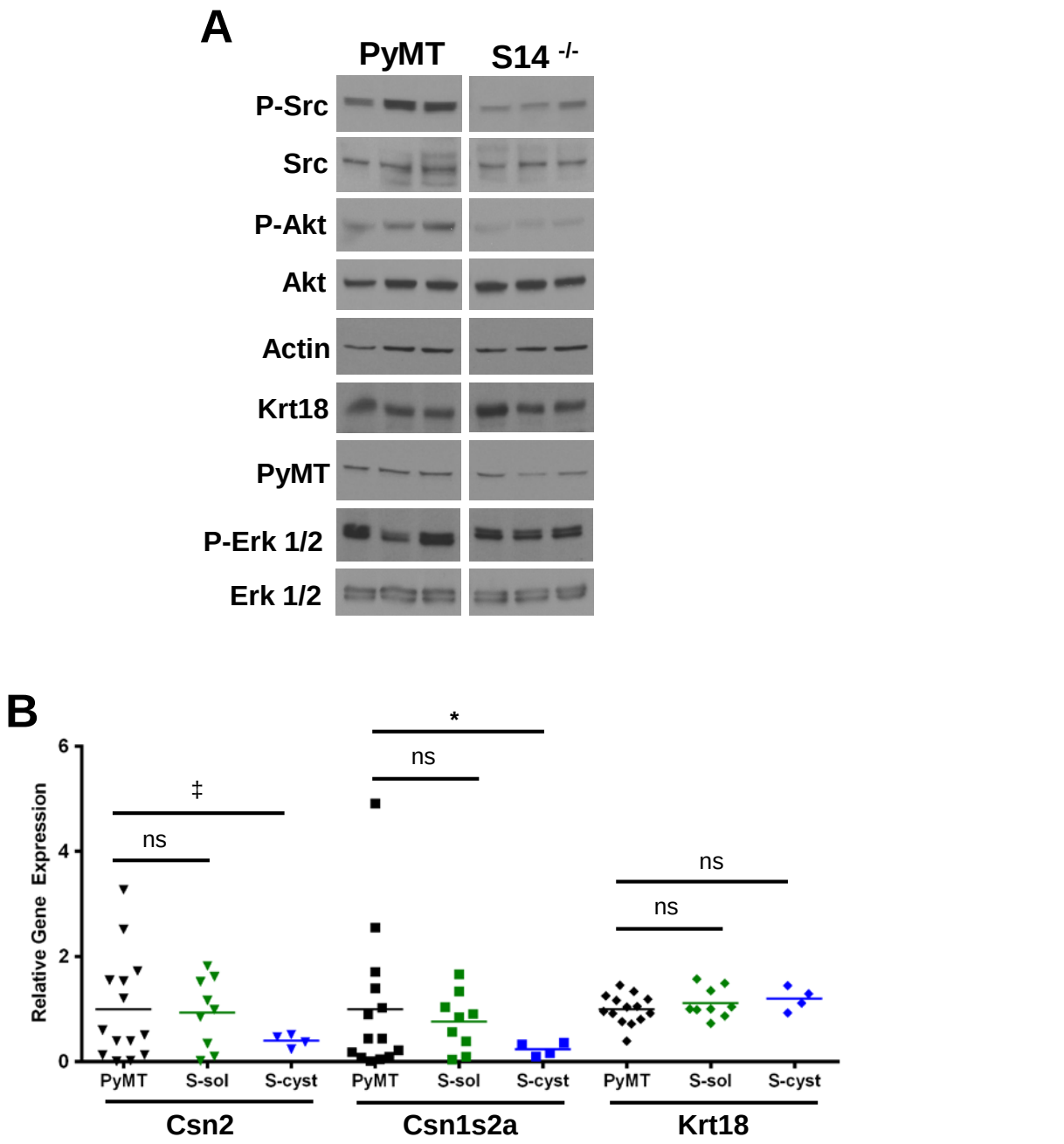

Figure 3. Analysis of solid tumors from PyMT and PyMT/S14$^{-/-}$ mice. A) Actin and keratin 18 (Krt18) are shown as loading controls. Phosphorylation sites evaluated for Src and Akt were P-Src Y416 and P-Akt S473 . B) QPCR analysis of tumors from PyMT and PyMT/S14-/- mice. Tumors from PyMT/S14-/- (S) mice are categorized as solid (S-sol; green) or cystic (S-cyst; blue). ‡ $p<0.1$; * $p<0.05$; ** $p<0.01$; ns = not significant.

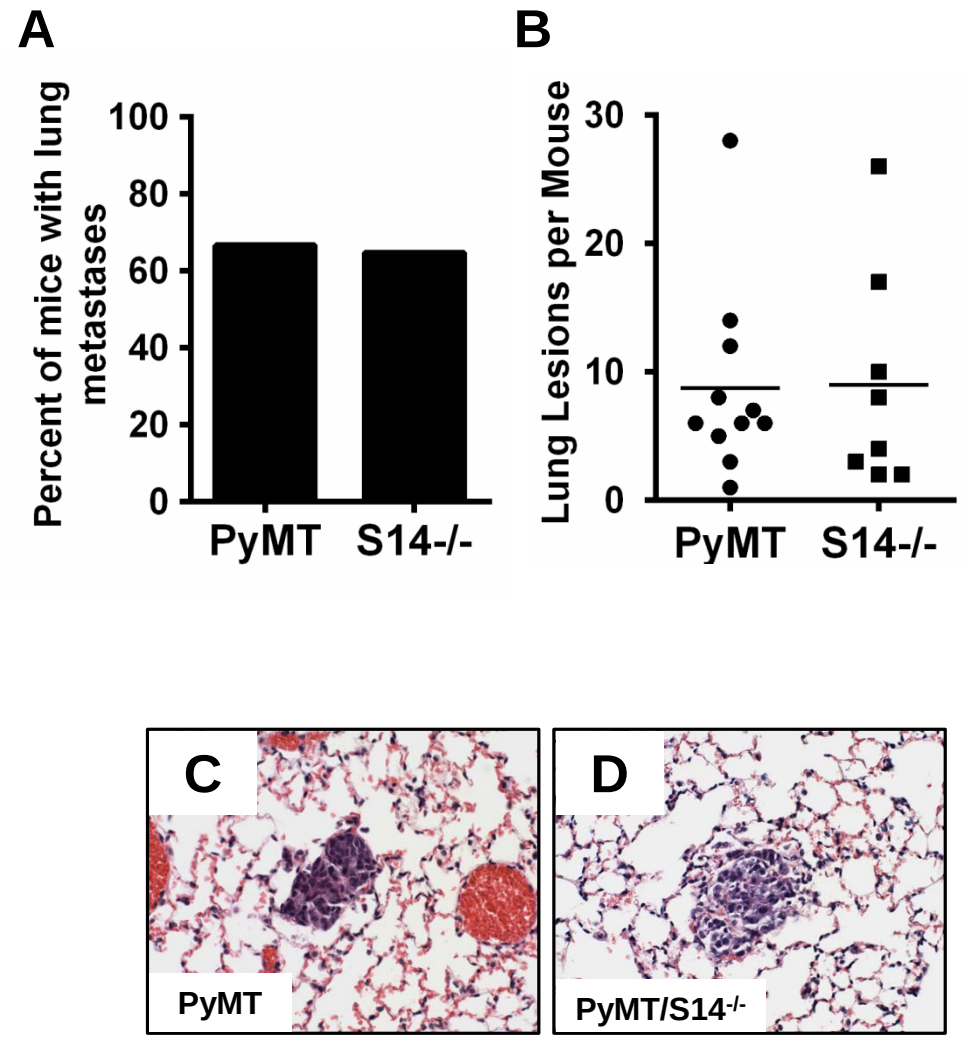

Figure 4. Influence of S14 loss on tumor metastasis. A) Percent of mice with visible lung metastases upon H&E examination in PyMT or PyMT/S14$^{-/-}$ (S14$^{-/-}$) mice. B) Number of visible lung lesions in PyMT or S14$^{-/-}$ mice. Representative metastatic lesions in lungs from PyMT (C) and S14$^{-/-}$ (D) mice captured at 40x magnification.

Table 1. GO Enrichment analysis of genes differentially expressed between PyMT and PyMT/S14-/- tumors.

Gene Ontology Term (Biological Process)	PValue	Fold Enrichment
glycolysis	0.0003	10.35
glucose catabolic process	0.0006	8.76
hexose catabolic process	0.0006	8.76
monosaccharide catabolic process	0.0007	8.43
cellular carbohydrate catabolic process	0.0011	7.59
alcohol catabolic process	0.0016	7.01
carbohydrate catabolic process	0.0042	5.62
fat-soluble vitamin metabolic process	0.0098	8.93
glucose metabolic process	0.0103	3.80
regulation of protein kinase activity	0.0113	3.26
positive regulation of cell proliferation	0.0126	2.67
vitamin metabolic process	0.0127	5.50
regulation of kinase activity	0.0133	3.16
response to DNA damage stimulus	0.0134	2.64
cell cycle	0.0145	1.99
oxidation reduction	0.0153	1.92
regulation of transferase activity	0.0160	3.05
generation of precursor metabolites and energy	0.0217	2.62
heterocycle catabolic process	0.0222	6.60
mitotic sister chromatid segregation	0.0228	12.65
hexose metabolic process	0.0239	3.14
sister chromatid segregation	0.0252	11.99
isoprenoid metabolic process	0.0262	6.20
negative regulation of cell activation	0.0321	5.73
negative regulation of leukocyte activation	0.0321	5.73
regulation of phosphorylation	0.0372	2.36
monosaccharide metabolic process	0.0399	2.78
mitotic cell cycle	0.0416	2.49
M phase of mitotic cell cycle	0.0425	2.74
regulation of phosphorus metabolic process	0.0448	2.27
regulation of phosphate metabolic process	0.0448	2.27
vitamin A metabolic process	0.0452	8.76

Table 2. KEGG pathway analysis of genes differentially expressed between PyMT and PyMT/S14-/- tumors.

KEGG Pathway	PValue	Fold Enrichment
Glycolysis / Gluconeogenesis	0.0018	6.66
Pentose phosphate pathway	0.0045	11.62
Cell cycle	0.0254	3.54
Starch and sucrose metabolism	0.0799	6.29
Fructose and mannose metabolism	0.0837	6.12

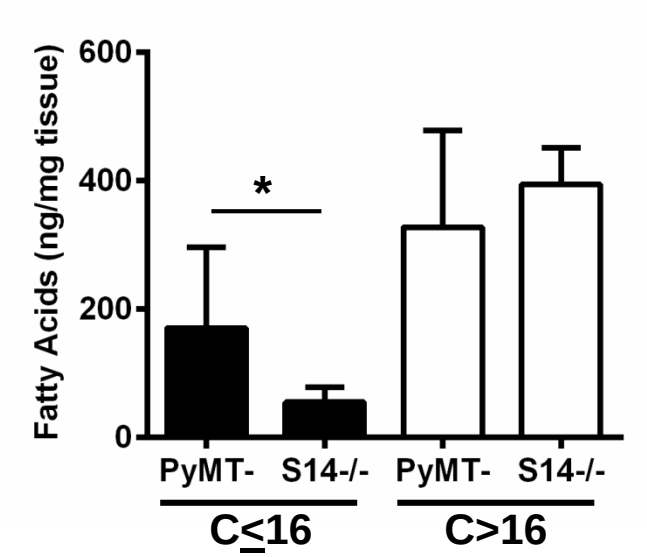

Figure 5. GC-Mass Spectrometry analysis of fatty acids. Tumor fatty acid contents from PyMT (N=6) and S14$^{-/-}$ (S14$^{-/-}$) (N=6) mice. Fatty acids are grouped according to chain length. Those with carbon chains $\leq$ 16 are on the left of the graph, and those with carbon chains > 16 are on the right of the graph.

Table 3. GC-Mass Spectrometry analysis of tumor fatty acid profiles.

Fatty Acid Chain Length and Saturation	Fatty Acids (ng per mg tissue)		Ratio S14-/- to PyMT	p-value	Fatty Acids (ng per mg tissue)		Ratio Neu/S14 to Neu	p-value
	PyMT	S14-/-			Neu	Neu/S14		
10:0	0.37	nd	0.00	0.113	5.65	19.14	3.39	0.068
12:0	2.75	nd	0.00	0.028	6.12	9.12	1.49	0.349
14:0	16.90	4.95	0.29	0.005	23.52	45.78	1.95	0.026
14:1	0.41	0.28	0.69	0.209	1.06	3.89	3.68	0.015
16:0	120.87	34.44	0.28	0.027	157.33	328.56	2.09	0.010
16:1	29.10	15.66	0.54	0.11	17.73	93.91	5.30	0.103
18:0	15.51	12.02	0.77	0.234	143.39	202.74	1.41	0.062
18:1	328.43	197.66	0.60	0.191	154.88	292.21	1.89	0.026
18:2	236.79	116.73	0.49	0.178	100.49	227.83	2.27	0.027
18:3	12.28	6.10	0.50	0.183	0.71	0.67	0.95	0.817
20:4	47.10	61.99	1.32	0.026	39.54	42.94	1.09	0.868

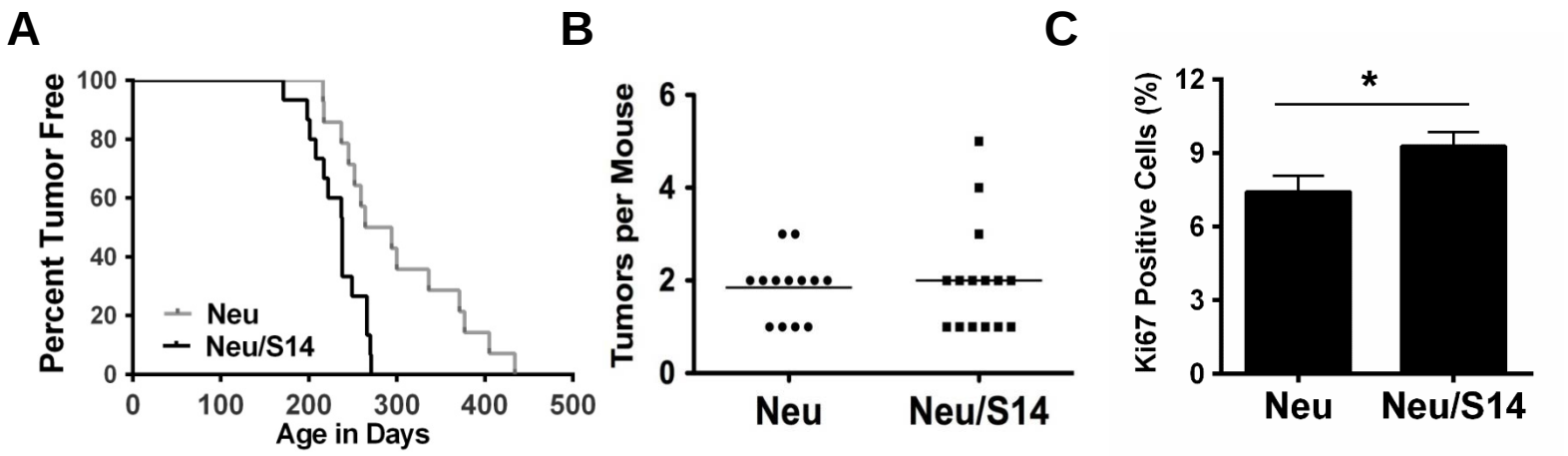

Figure 6. Tumor latency, multiplicity, and proliferation in Neu and Neu/S14 mice. A) Kaplan Meier survival curve of tumor latency in Neu and Neu/S14 mice. Median times to tumor onset were 238 days (Neu/S14) and 279 days (Neu); HR 3.781 (1.554-9.202); Log rank pvalue = 0.0034. B) Number of tumors per mouse at sacrifice. C) Quantification of Ki67 IHC (number of positive nuclei out of total) in tumors; p=0.02

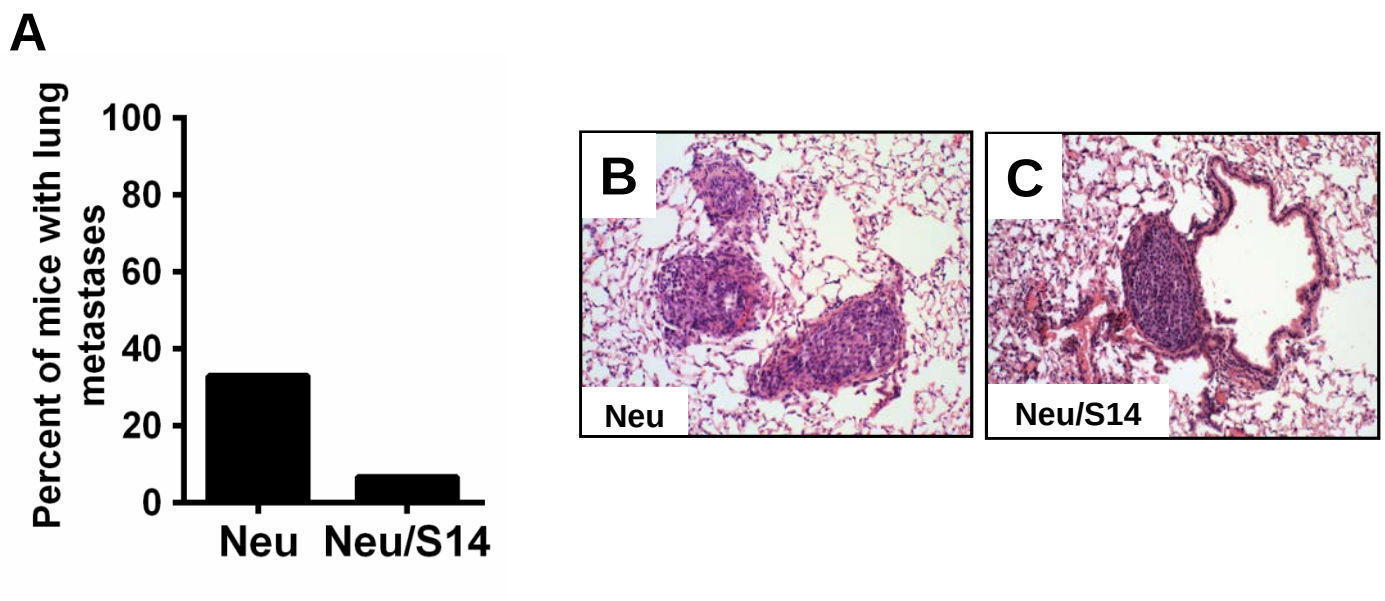

Figure 7. Influence of S14 overexpression on tumor metastasis. A) Percent of mice with visible lung metastases upon H&E examination in Neu or Neu/S14 mice. Representative metastatic lesions in lungs from Neu (B) and Neu/S14 (C) mice. (B) and (C) were captured at 20x magnification.

Table 4. GO Enrichment analysis of genes differentially expressed between Neu and Neu/S14 tumors.

Gene Ontology Term (Biological Process)	PValue	Fold Enrichment
translation	2.55E-05	2.34
positive regulation of growth	0.0021	3.87
cellular response to stress	0.0030	1.79
heart morphogenesis	0.0034	3.25
in utero embryonic development	0.0038	1.98
regulation of cell proliferation	0.0057	1.61
regulation of cell cycle	0.0080	2.02
macromolecular complex subunit organization	0.0106	1.70
heart development	0.0118	1.94
heterophilic cell adhesion	0.0118	5.47
cellular macromolecular complex subunit organization	0.0138	1.87
vacuolar transport	0.0139	5.23
macromolecular complex assembly	0.0140	1.71
positive regulation of developmental growth	0.0149	7.40
protein folding	0.0166	2.27
electron transport chain	0.0180	2.36
ribosome biogenesis	0.0180	2.36
cellular macromolecular complex assembly	0.0189	1.88
homotypic cell-cell adhesion	0.0231	12.02
blastocyst development	0.0238	3.12
DNA packaging	0.0243	2.38
negative regulation of cell proliferation	0.0247	1.83
negative regulation of programmed cell death	0.0260	1.77
negative regulation of cell death	0.0269	1.77
regulation of programmed cell death	0.0271	1.46
ribonucleoprotein complex biogenesis	0.0273	2.11
chordate embryonic development	0.0282	1.54
regulation of cell death	0.0289	1.45
regulation of striated muscle tissue development	0.0290	3.44
ER to Golgi vesicle-mediated transport	0.0306	4.15
regulation of cellular component biogenesis	0.0313	2.43
embryonic development ending in birth or egg hatching	0.0314	1.53
regulation of muscle development	0.0318	3.36
oxidation reduction	0.0324	1.40
immunoglobulin production	0.0342	4.01
chromatin assembly	0.0357	2.57
regulation of apoptosis	0.0363	1.44
somatic recombination of immunoglobulin gene segments	0.0365	5.34
RNA biosynthetic process	0.0368	2.10
cell-cell adhesion	0.0374	1.73
nucleosome organization	0.0380	2.53
protein-DNA complex assembly	0.0380	2.53
aging	0.0402	2.76
determination of adult life span	0.0408	9.02
purine nucleoside triphosphate catabolic process	0.0408	9.02
negative regulation of apoptosis	0.0411	1.71
regulation of cell adhesion	0.0413	2.30
production of molecular mediator of immune response	0.0421	3.76
negative regulation of nucleobase, nucleoside, nucleotide and nucleic acid metabolic process	0.0423	1.51
limbic system development	0.0464	3.64
negative regulation of nitrogen compound metabolic process	0.0465	1.50
nitrogen compound biosynthetic process	0.0474	1.59
somatic diversification of immunoglobulins	0.0480	4.81
blood vessel development	0.0482	1.68

Table 5. KEGG pathway analysis of genes differentially expressed between Neu/S14 and Neu tumors.

KEGG Pathway	PValue	Fold Enrichment
Ribosome	0.0001	3.76
Oxidative phosphorylation	0.0043	2.57
Colorectal cancer	0.0479	2.39
Arginine and proline metabolism	0.0528	2.91
Pyrimidine metabolism	0.0773	2.14
RNA degradation	0.0813	2.57
O-Glycan biosynthesis	0.0846	3.81
Amino sugar and nucleotide sugar metabolism	0.0889	2.92

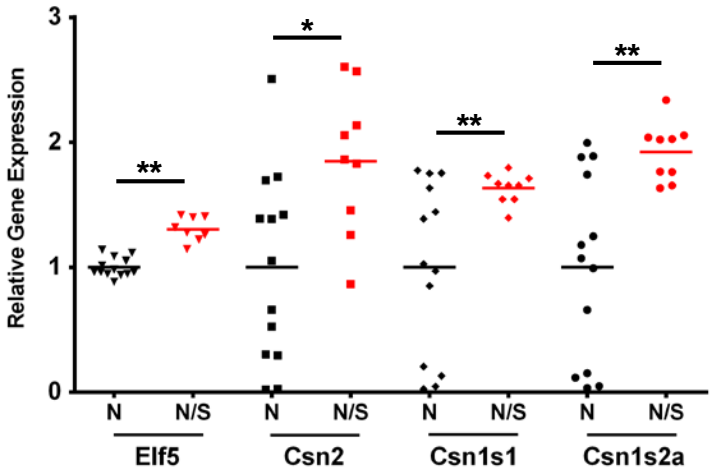

Figure 8. Expression of genes associated with mammary epithelial cell differentiation in primary tumors from Neu (N; black) and Neu/S14 (N/S; red) mice.

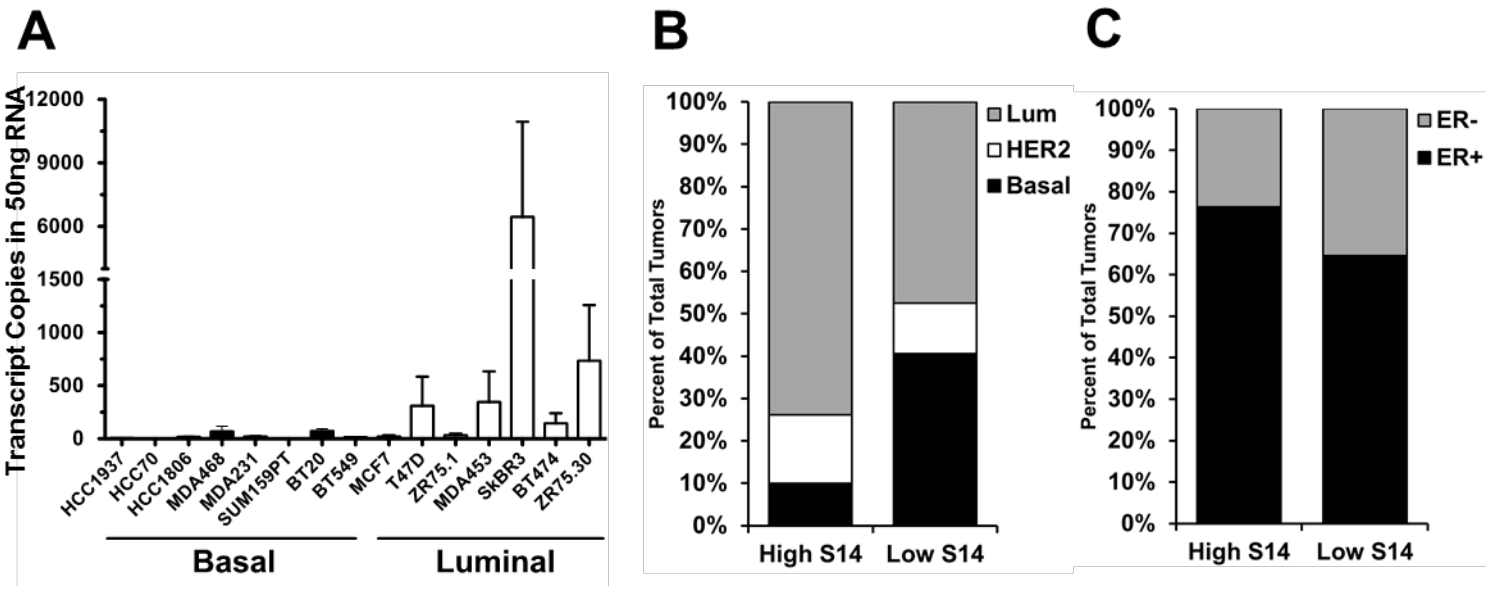

Figure 9. Association between S14 and human breast tumor differentiation markers. A) S14 expression in human breast cancer cells, measured as transcript copies in 50 ng RNA. B) Tumors with High S14 (N=192) are more likely to be luminal versus basal (p=0.0002) compared to tumors with Low S14 (N=204). C) Tumors with High S14 (N=436) are more likely to be ER+ versus ER- (p<0.0001) than tumors with Low S14 (N=438).

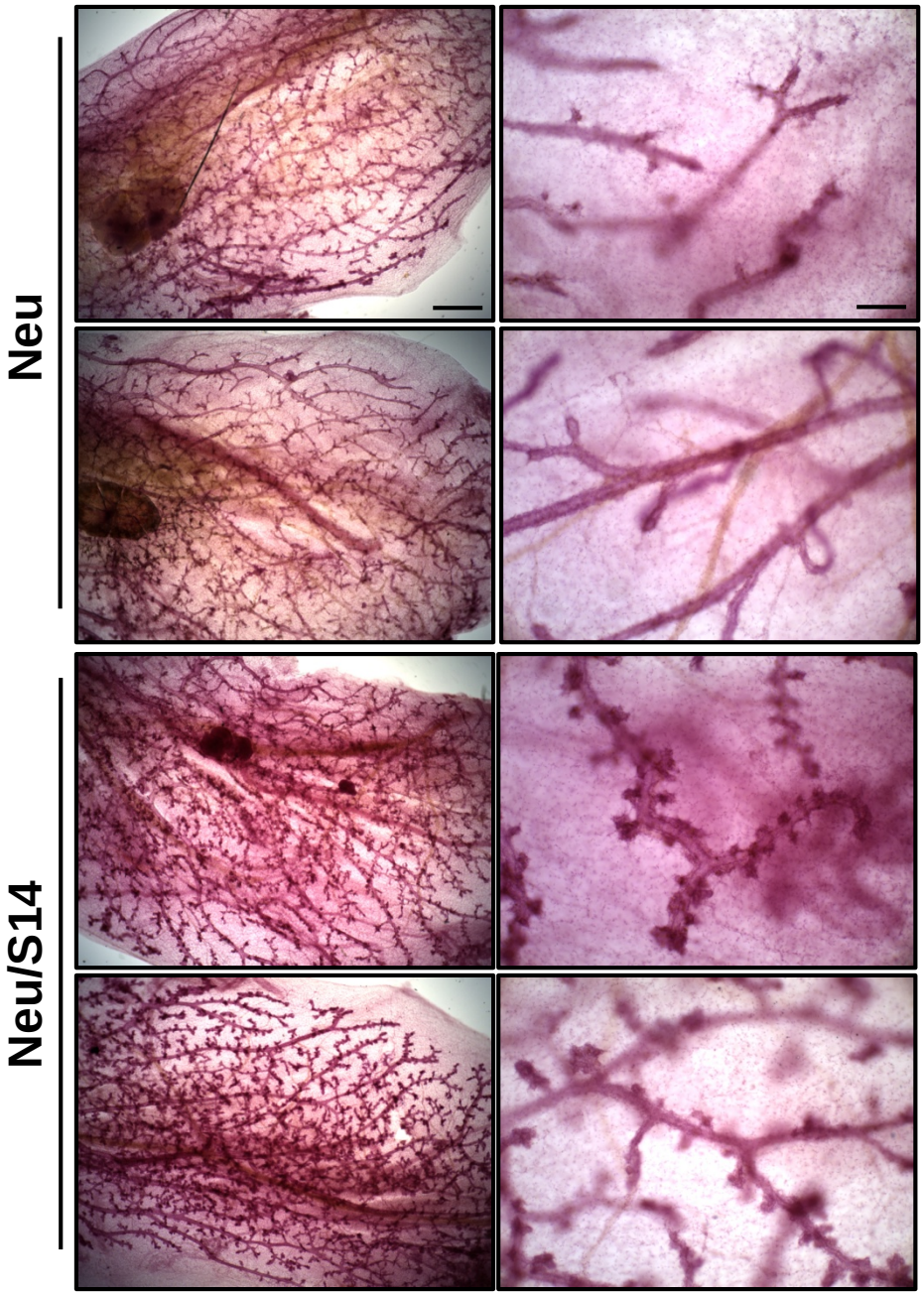

Figure 10. Morphology of non-tumor bearing mammary glands from Neu and Neu/S14 mice. **W**hole mounted mammary glands from N=2 each Neu and Neu/S14 mice at 10 months of age and in diestrus. Scale for left column (2x) is 1 mm, scale for right column (10x) is 200 µm.

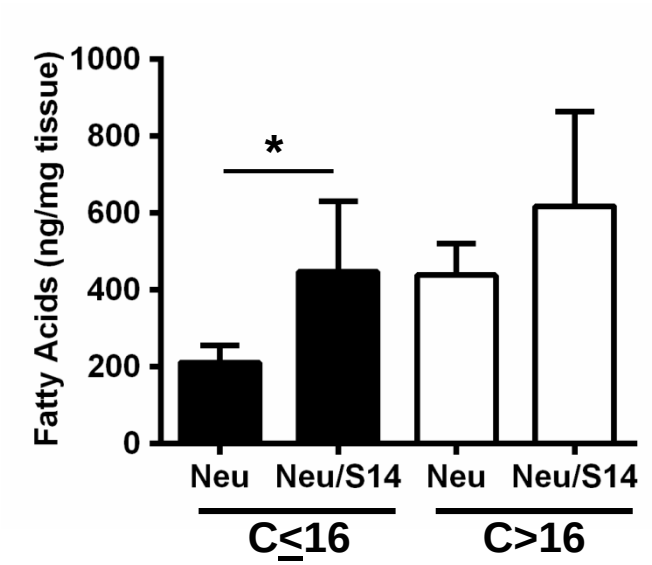

Figure 11. GC-Mass Spectrometry analysis of fatty acids. Tumor fatty acid contents from Neu (N=8) and Neu/S14 (N=7) mice. Fatty acids are grouped according to chain length. Those with carbon chains ≤ 16 are on the left of the graph, and those with carbon chains > 16 are on the right of the graph.

Salaried Personnell: Elizabeth Wellberg was the only personnell to receive salary from this funding source.

Key Research Accomplishments

- We have generated MMTV-Neu/MMTV-Spot14 (Neu/S14) mice and have completed the study on mammary tumorigenesis.
- From the above model, we have demonstrated a role for Spot14 in stimulating the formation of Neu-induced mammary tumors and enhancing cell proliferation within those tumors.
- We have performed NMR, GC-mass spec, and microarray analyses on tumors from experimental and control groups and have shown that Neu/S14 tumors are well-differentiated, as they display hallmarks of the lactating mammary gland.
- We have shown that Neu/S14 tumors have elevated fatty acid contents, but that this is not sufficient to increas metastasis as we had previously suspected.
- I have learned to perform bioinformatics analysis of public human tumor datasets and metadata and have used these tools to support the studies performed in our mouse model.
- We have generated MMTV-PyMT/Spot14-null mice and have completed the study on mammary tumorigenesis in this model.
- We have shown that loss of Spot14 decreases fatty acid synthesis and tumor growth in vivo.

Reportable Outcomes

A manuscript describing the results of our mouse studies, investigating the role of Spot14 in mammary tumorigenesis and fatty acid synthesis, is currently under review at Breast Cancer Research.

This study allowed us to generate microarray data, comparing tumors with Spot14 overexpression and Spot14 loss to their respective controls. These studies were deposited into the NCBI Gene Expression Omnibus (GEO) database for access by all researchers.

The results of these studies have been presented at one or more meetings annually for discussion with colleagues and collaborators.

Based on these studies, we have submitted proposals to the NIH (NCI) and the DoDBCRP to evaluate the effects of de novo synthesized versus preformed fatty acids on mammary tumorigenesis.

Conclusion

This study was the first to identify a role for Spot14 in the growth, metabolism, and metastasis of mammary tumors in vivo. We showed that overexpression of Spot14 accelerated the formation of Neu-induced mammary tumors, which was associated with elevated tumor cell proliferation

and increased tumor de novo fatty acid synthesis. We also showed that loss of Spot14 from PyMT-driven mammary tumors decreased the growth rates of these tumors and also decreased tumor de novo fatty acid synthesis. Using computational biology, we identified a novel link between high Spot14 and the luminal subtype of human breast cancer, which we confirmed in our mouse models. Overall, our studies suggest that elevated tumor de novo fatty acid synthesis is both necessary and sufficient to support tumor growth and suggests a closer look is necessary into the role of Spot14 in luminal tumor cell differentiation before designing therapeutics against it.

Why does this matter?

The mechanisms through which tumor cells reprogram their metabolism to accomplish un-checked proliferation are numerous. In addition to upregulating glucose metabolism and altering the way they use the Citric Acid cycle in the mitochondria, tumor cells also increase de novo fatty acid synthesis. This is thought to accomplish several goals for the tumor, including the production of new cell membranes as cells divide. The conundrum is that, with few exceptions, people consume more than enough fat for tumors to use what is circulating in the blood. Yet they still increase the activity of Fatty Acid Synthase (FASN). One way that we think that breast cancers do this is by increasing Spot14 levels, which we have shown to activate the FASN enzyme. This suggests that Spot14 is a potential target for breast cancer therapy, and our data suggest that this may be so particularly in tumors from the luminal subtype, which represent the majority of breast tumors. More importantly, this study has identified a role for de novo synthesized fatty acids in tumor growth. This suggests that the fatty acids that are made by the tumor cell have some greater purpose than just providing lipids for membrane biogenesis, or else the dietary fats would suffice. If we can target the de novo fatty acid synthesis pathway, this could offer a therapeutic opportunity for many cancer types.

Meeting Abstracts in bibliography form

Wellberg EA, Rudolph MC, Lewis A, and Anderson SM. THRSP/Spot14 regulates mammary tumor growth and fatty acid synthesis. Presented at the Endocrine Society Conference in June, 2011.

Wellberg EA, Rudolph MC, Lewis A, and Anderson SM. THRSP/S14 accelerates mammary tumor formation and enhances cell proliferation in MMTV-Neu mice. Presented at the Mammary Gland Biology Program Project Grant Annual Retreat in February, 2012.

Wellberg EA, Rudolph MC, Lewis A, and Anderson SM. THRSP/S14 accelerates mammary tumor formation and enhances cell proliferation in MMTV-Neu mice. Presented at the Endocrine Society Conference in June, 2012.

Wellberg EA, Rudolph MC, Lewis A, Padilla NJ, Jedlicka P, and Anderson SM. Dual Role of Spot14 In Mammary Tumorigenesis: Spot14 Increases Tumor Growth But Reduces Tumor

Metastasis By Influencing Mammary Lobular Differentiation. Presented at the Mammary Gland Biology Gordon Research Conference in June, 2013.

Wellberg EA, Rudolph MC, Lewis A, and Anderson SM. Regulation of mammary tumorigenesis and fatty acid synthesis by Spot14. Presented at the Mammary Gland Biology Program Project Grant Annual Retreat in February, 2014.

Wellberg EA, Rudolph MC, Lewis A, and Anderson SM. Stimulation of fatty acid synthesis by Spot14 enhances tumor cell proliferation in vivo. Presented at the AACR Conference in October 2014.

References

1. Guy CT, Cardiff RD, Muller WJ. Induction of mammary tumors by expression of polyomavirus middle T oncogene: a transgenic mouse model for metastatic disease. Mol Cell Biol 1992;12(3): 954-61.

2. Dilworth SM. Polyoma virus middle T antigen and its role in identifying cancer-related molecules. Nat Rev Cancer 2002;2(12): 951-6.

3. Hebbard L, Cecena G, Golas J, et al. Control of mammary tumor differentiation by SKI-606 (bosutinib). Oncogene 2011;30(3): 301-12.

4. Rudolph MC, Wellberg, E. A., Lewis, A. S., Terrell, K. L., Merz, A. L., Maluf, N. K., Serkova, N. J., and Anderson, S. M. Thyroid Hormone Responsive Protein Spot14 Enhances Catalysis of Fatty Acid Synthase in Lactating Mammary Epithelium. Journal of Lipid Research.

5. Guy CT, Webster MA, Schaller M, Parsons TJ, Cardiff RD, Muller WJ. Expression of the neu protooncogene in the mammary epithelium of transgenic mice induces metastatic disease. Proc Natl Acad Sci U S A 1992;89(22): 10578-82.

6. Kouros-Mehr H, Bechis SK, Slorach EM, et al. GATA-3 links tumor differentiation and dissemination in a luminal breast cancer model. Cancer Cell 2008;13(2): 141-52.

7. Harris J, Stanford PM, Sutherland K, et al. Socs2 and elf5 mediate prolactin-induced mammary gland development. Mol Endocrinol 2006;20(5): 1177-87.

8. Chakrabarti R, Hwang J, Andres Blanco M, et al. Elf5 inhibits the epithelial-mesenchymal transition in mammary gland development and breast cancer metastasis by transcriptionally repressing Snail2. Nat Cell Biol 2012;14(11): 1212-22.

9. Perou CM, Sorlie T, Eisen MB, et al. Molecular portraits of human breast tumours. Nature 2000;406(6797): 747-52.